U.S. DEPARTMENT OF THE INTERIOR

U.S. GEOLOGICAL SURVEY

ELECTRICAL RESISTIVITY SURVEY IN THE CORNUDAS MOUNTAINS AREA, OTERO COUNTY, NEW MEXICO

by

Douglas P. Klein and Brian D. Rodriguez

U.S. Geological Survey
Denver, Colorado

Open-File Report 97-149

1997

ELECTRICAL RESISTIVITY SURVEY IN THE CORNUDAS MOUNTAINS AREA, OTERO COUNTY, NEW MEXICO

Douglas P. Klein and Brian D. Rodriguez
U.S. Geological Survey
1997

INTRODUCTION

Electrical geophysical data were acquired in the Cornudas Mountains area of southern New Mexico in April, 1996, using the audio-magnetotelluric (AMT) method. Natural variations in the electric and magnetic fields at the surface of the Earth were observed at 8 locations spaced at distances of 11 to 26 km apart to provide a reconnaissance of the subsurface resistivity in that area. The data were acquired across a range of frequencies from 4.5 to 27,000 Hz, and were interpreted to provide estimates of the Earth's resistivity at depths from about 5 to 2,200 m beneath the surface.

Electrical resistivity of the Earth is dependent on the fabric, composition, water content, and temperature of rocks sensed; with this basis, the purpose of the survey was to assist in the geological investigation of the Cornudas Mountains area for the Bureau of Land Management (BLM). This work is part of a U.S. Geological Survey (USGS) mineral-environmental investigation of the Caballo Resource area, an area that includes Sierra and Otero Counties, New Mexico.

The area of investigation is located in Otero County, New Mexico near the New Mexico-Texas border within Townships T25S to T26S and Ranges R13E to R16E. The Cornudas Mountains here consist of a group of rounded peaks composed of Tertiary syenitic intrusions that emerge from a plain underlain by Permian and Early

Cretaceous limestone and other sedimentary rocks (McLemore and Guilinger, 1995). The area has been explored for gold, silver, beryllium, rare earth elements, and nepheline syenite. There is interest is in the nepheline syenite for use in glass, ceramic products, and abrasives (McLemore and Guilinger, 1995; U.S. Bureau Mines, 1994).

Intrusions of the Cornudas Mountains are predominately unaltered and are associated with highs in the magnetic field as mapped from aeromagnetic surveys. At Wind mountain, for instance, the zone of contact alteration between the Wind Mountain syenite and it's host rock is only about 2 to 5 meters wide. Unaltered intrusions usually show high resistivity compared to shale- or clay-bearing sedimentary rocks. One goal of the present work was to see if any high resistivity subsurface bodies could be detected, and if so, are they preferentially associated with rocks beneath magnetic highs. Such combined evidence could point to shallow intrusions beneath the surface in areas where outcrop is lacking. Also, the intrusions have deformed their host rocks during emplacement. The resulting change in rock structure may have a signature in electrical resistivity because of the opening of rock fractures and the subsequent presence of small amounts of pore water and alteration in these fractures which would lower the resistivity. Besides detection of deformation halos, broader changes in structure or lithology may be detected from lateral changes in thickness and resistivity of various rock units.

DATA

AMT surveys utilize naturally occurring time-variations in electric (E) and magnetic (H) fields that are measured across electrically grounded lines and through induction coils respectively. Electric and magnetic fields were measured in two horizontal, orthogonal, directions giving data for 4 components.

The relationship between horizontal and orthogonal E and H for given frequencies is determined by the resistively (or conductivity, the inverse of resistivity) of the Earth (Vozoff, 1972, 1991; Strangeway and others, 1973).

The depth of investigation for electromagnetic fields is dependent on the ratio of resistivity/frequency, such that for a given resistivity, lower frequencies give information at greater depth. For the present study, data were acquired at 14 logarithmically separated frequencies from 4.5 to 27,000 Hz. These different frequencies allow the data to interpreted for resistivity through a range of depths; for the present study this range was 5 to 2,200 m. In addition, the two sets of orthogonal E:H fields acquired with AMT data may indicate lateral changes in resistivity caused by anisotropy or structure in the subsurface resistivity.

Instrumentation for this study was originally designed and built by the USGS for geothermal studies (Hoover and Long, 1976; Hoover and others, 1978). The receiver uses envelope-peak detection of signal amplitudes at specific frequencies defined by narrow, band-pass filters (ratio of central frequency to band-width is 50). The means of data acquisition was to record the peaks on chart paper. In this analog recording, the data contain only amplitude information.

A 1995 modification to the instrumentation, used for the present survey, was the replacement of the analog recorders by an 4-channel, 12-bit, microprocessor-controlled, digitizer (T. Grover, USGS, Denver, unpublished documentation, 1996; currently at Colorado School of Mines, Golden). This digitizer captures signals at a selected band-pass frequency after gain and filtering have been applied; data are transferred to a PC-compatible, field computer for display, analysis, and storage.

Digitizer operation is controlled by a field computer to allow various options during data acquisition. The operator sets sampling rates at various values from 32 to 250,000 Hz, and the length of data series at a value of 256, 512, or 1024 samples. AMT signals arise chiefly from atmospheric disturbances, such as distant lightening strokes, thus the signals tend to be impulsive, and may be polarized. The digitizer has operator controlled options to select criteria for which to record 'events' (impulses) based on relative signal amplitude and correlation among the acquired AMT fields at the selected frequency. Data are continuously stored and replaced in circular buffers in the digitizer, so that a recorded time series matching the selection criteria has equal sampling lengths on either side of the center of an event.

The present survey was the first field application of the digitizer described above. PC-based software for processing the data was under development as the work reported here progressed.

The survey procedure was to collect 3 to 6 time-series of 512 samples for each channel and each mode (Ex:Hy and Ey:Hx). Events were selected if there was correlation between the components of each mode, and if event amplitudes exceeded 10- to 40-percent of the recording range, dependent on amplitudes at the acquisition frequency. Background signals and noise were typically 5- to 20-percent full-scale, with occasional larger events. Processing used Fourier analysis. The signal components were estimated by averaging 3 to 5 Fourier harmonics centered on the central frequency of the time-series, and combining these harmonics into auto- and cross-spectra. Some events correlating in Ex:Hy had weak to poor signals in Hy:Ex and vice versa; therefore, the Ex:Hy and Ey:Hx modes were processed separately. Cross-spectra were converted to apparent resistivity units (Ohm-m), and E:H phase for each mode and frequency (Vozoff, 1972). If the Earth were uniform, then apparent resistivity would be constant for all frequencies and would be equal to the Earth's resistivity, and all phases would be 45 degrees. Usually, apparent resistivity and phase change with frequency indicating non-uniformity with depth. Apparent resistivity may also vary between E:H directions as a function of frequency; the cane indicate lateral non-uniformity at various depths. For these reasons, apparent resistivity data have to be interpreted using forward modeling or inversion to estimate the Earth's resistivity distribution (Vozoff, 1972, 1991).

Graphs of apparent resistivity versus frequency (sounding curves) are presented in the Appendix, along with a theoretical curve for a representative model of resistivity versus depth for each station. The apparent resistivity data often display scatter greater than 10-percent on a logarithm scale. This noise is due to the early stages of processing software, windy conditions encountered during the survey, and electromagnetic contamination from cultural signals (such as local power and telephone line signals) that adversely influenced some of the data.

RESULTS

Sounding locations (Figure 1) were in part guided by aeromagnetic anomalies based on a premise that the syenitic intrusions may have an aeromagnetic expression. Wind Mountain, for instance, is associated with an aeromagnetic high of about 300 nT amplitude. Other aeromagnetic anomalies in the area with smaller amplitudes may also indicate buried intrusions. Observations were not limited to aeromagnetic highs; the object of this survey was partly to establish a broad areal resistivity signature of the area. The results show no consistent correlation between the resistivity at depth and the aeromagnetic signature, but they do provide a guide to the main characteristics of the resistivity distribution in the area.

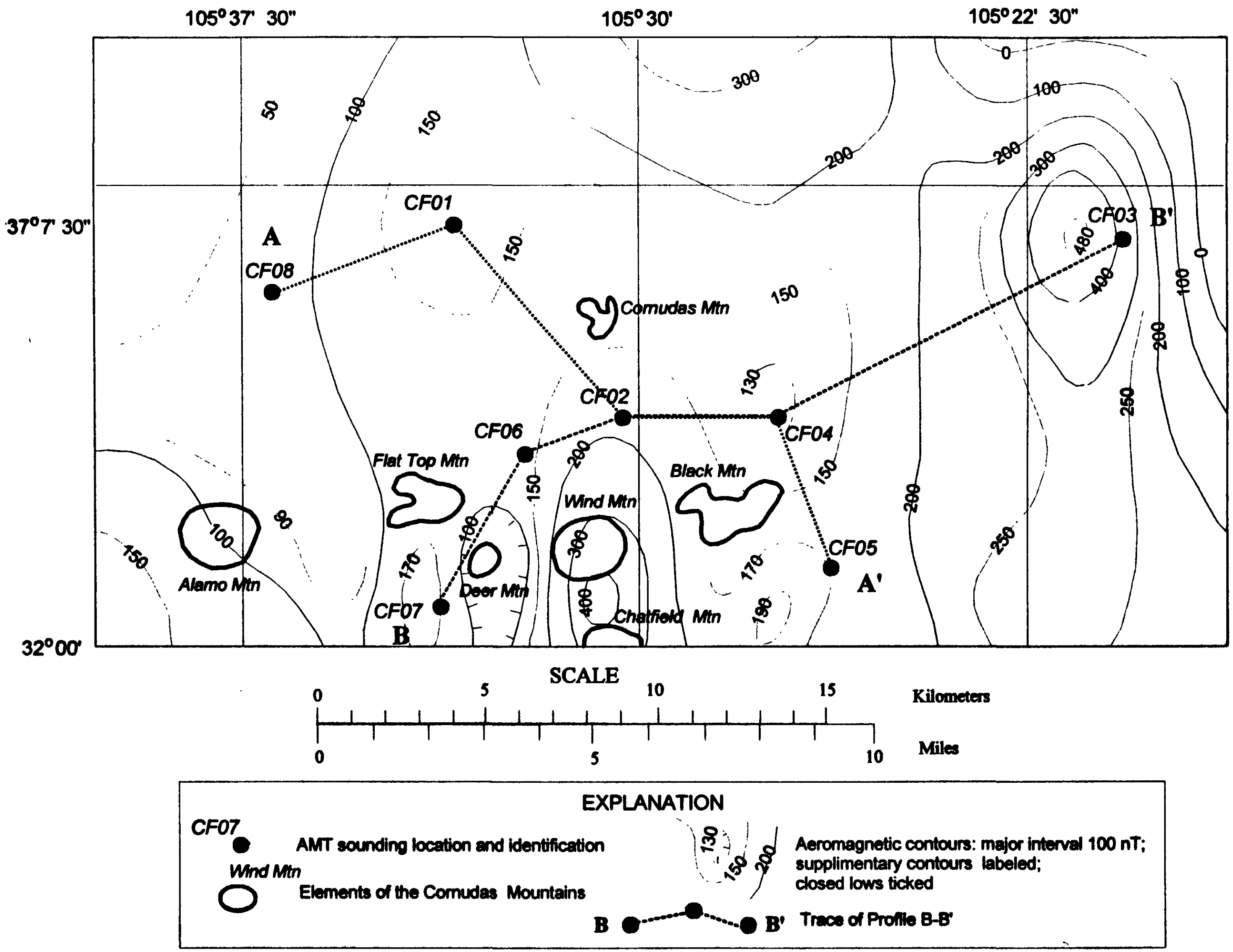

Figure 1 -- Location of AMT sounding stations (CF01 to CF08) in the Cornudas Mountains area. southern New Mexico. Contours show aeromagnetic anomaly values from a preliminary unpublished compilation (Dean Kleinkopf, USGS, Denver, April, 1996; data from Cordell 1983)

Table 1 summarizes the results from AMT observations for each station (see the Appendix for data plots). The estimated resistivity beneath each station is based on comparing theoretical data from various models to the observed data. The models are composed of 2 to 4 discrete horizontal layers; calculations of the theoretical data are based on an algorithm similar to those described by Wait (1962), and Madden and Nelson (1985). The "data quality" column in Table 1 is a qualitative descriptor. Data are considered good to fair when the scatter (change) among apparent resistivity estimates at nearby frequencies is about 10- to 30-percent log cycle. The models (Appendix), provide a basis against which to consider scatter. For a layered Earth, the maximum change of apparent resistivity on a log-log sounding curve plot is equal to the change in frequency. The layered Earth assumption is valid if lateral changes in resistivity are negligible within a radius of the depth of penetration.

Most models can be considered approximate estimates of the Earth resistivity; variations of about 10- to 30-percent in resistivity or depth from these models would probably be equally acceptable at many stations. Resistivity values greater than about 10,000 Ohm-m for some of the layers are not considered realistic, but, never-the-less, provided the better fitting models generated during forward modeling.

Table 1 -- Summary of results from AMT soundings in the Cornudas Mountains area. The thickness of the deepest layer in all case is indefinite. The data quality column provides a subjective qualifier, based on scatter and how well a layered resistivity model fits the data. Resistivity values greater than 10,000 Ohm-m are questionable, but indicate high resistivity.

STA.	**DATA QUALITY**	**LAYER RESISTIVITY (Ohm-m)**	**LAYER THICKNESS (m)**	**REMARKS**
CF01	good	15 1000 30	10 400	On a broad 30 nT aeromagnetic high
CF02	very poor	15 200,000	10	On the north end of the Wind Mountain aeromagnetic high
CF03	poor	500 50,000 500 500,000	50 2,000 200	On flank of 1000 nT aeromagnetic high; broad topographic high
CF04	poor	20 10,000	20	On broad 20 nT aeromagnetic low; minor topography
CF05	good	20 1000 10 1000	3 200 50	On flank of 30 nT aeromagnetic low; minor topography
CF06	fair	50 1,000 10	20 100	On northwest flank of Wind Mountain aeromagnetic high
CF07	fair	10 1000 3	10 100	On 30 nT aeromagnetic high southwest of Deer Mountain
CF08	fair	10 1,000 1 30	5 200 30	On plains west of topography and aeromagnetic anomalies

Results from all soundings, except stations 3 and 5, indicate that the area is characterized by a profile of low/high/low resistivity. The 1^{st} low-resistivity layer, with a thickness of a few to few-tens of meters, has a resistivity of typically 5 to 50 Ohm-m, but up to 500 Ohm-m at station 3. The 2^{nd} resistive layer, with thickness of a few hundreds of meters to a few thousand meters, has resistivity of 100 to 1,000 Ohm-m, or greater. The 3^{rd} low-resistivity layer has resistivity of 1-500 Ohm-m. This conductive 3^{rd} layer was not distinguished at stations 2 and 4. Exceptions to this low/high/low profile are also found in additional deep layers modeled at stations 3 and 5 in the eastern part of the study area.

The characteristic resistivity picture outlined above is in accord with a conductive weathered zone (1^{st} layer) of otherwise generally high resistivity (2^{nd} layer) rock. One may infer the 2^{nd} layer to be the signature of predominantly resistive limestone with variable amounts of shale, calcareous sandstone, and evaporites as indicated by surface exposures and in drill holes (Black, 1975; King and Harder, 1985; McLemore and Guilinger, 1995). This high resistivity could also be geophysically compatible with igneous or metamorphic rock, thus sills in carbonate rocks may be consistent with the character of the 2^{nd} layer. A drill hole description from Union-McMillion No. 1A (Section 9, T25S, R13E), about 8 km west of Cornudas Mountain, indicates about 30 m of sandstone and sandy carbonate rocks, overlaying 800 m of lower Permian red beds and gypsum (Black, 1975; King and Harder, 1985). In this borehole, the base of the Permian beds are composed of mudstone, muddy limestone, and shale. The conductive 3^{rd} layer may be produced by such mudstone and shale. An interpretive geologic structure section (Black, 1975; King and Harder, 1985) shows that the sedimentary section just described is present west of the Cornudas Mountains. The Mountains themselves are interpreted as projections from of a broad laccolith whose depth may be as shallow as some 10's of meters.

laccolith whose depth may be as shallow as some 10's of meters. The interpretative section (Black, 1975; King and Harder, 1985) also shows pre-Permian horsts and grabens east of the Cornudas Mountains that alternates Precambrian basement rock with older Paleozoic sedimentary rock below the Permian strata.

Two profiles showing the subsurface resistivity are shown on figure 2. There is a vertical exaggeration of 500 in these profiles. Station spacing was too great to confidently interpolate between stations, however, some broad features related to the structural configuration and intrusions in the Cornudas area may be inferred.

On the western side of the Cornudas area, the inferred carbonate rocks (1000 Ohm-m of the 2nd layer) is about 50 m thicker at station 8 compared to stations 6 and 7 in the more southerly part of the study area. The data also show a 350-m increase in the thickness of the 1,000 Ohm-m layer from station 8 to station 1 on profile A-A'. Interpretations to consider for these observations are structural warping, or sill intrusions in the 2nd (resistive) layer.

In the central part of the Cornudas area, soundings 1 and 6, compared to 2 and 4, suggest that the conductive 3rd layer disappears to the east of Wind and Cornudas Mountains, and possibly that the 2nd layer increases in resistivity. An igneous intrusion into the 2nd layer would increase it's resistivity, however, a decrease of shale or mudstone in the carbonate rocks would have a similar effect.

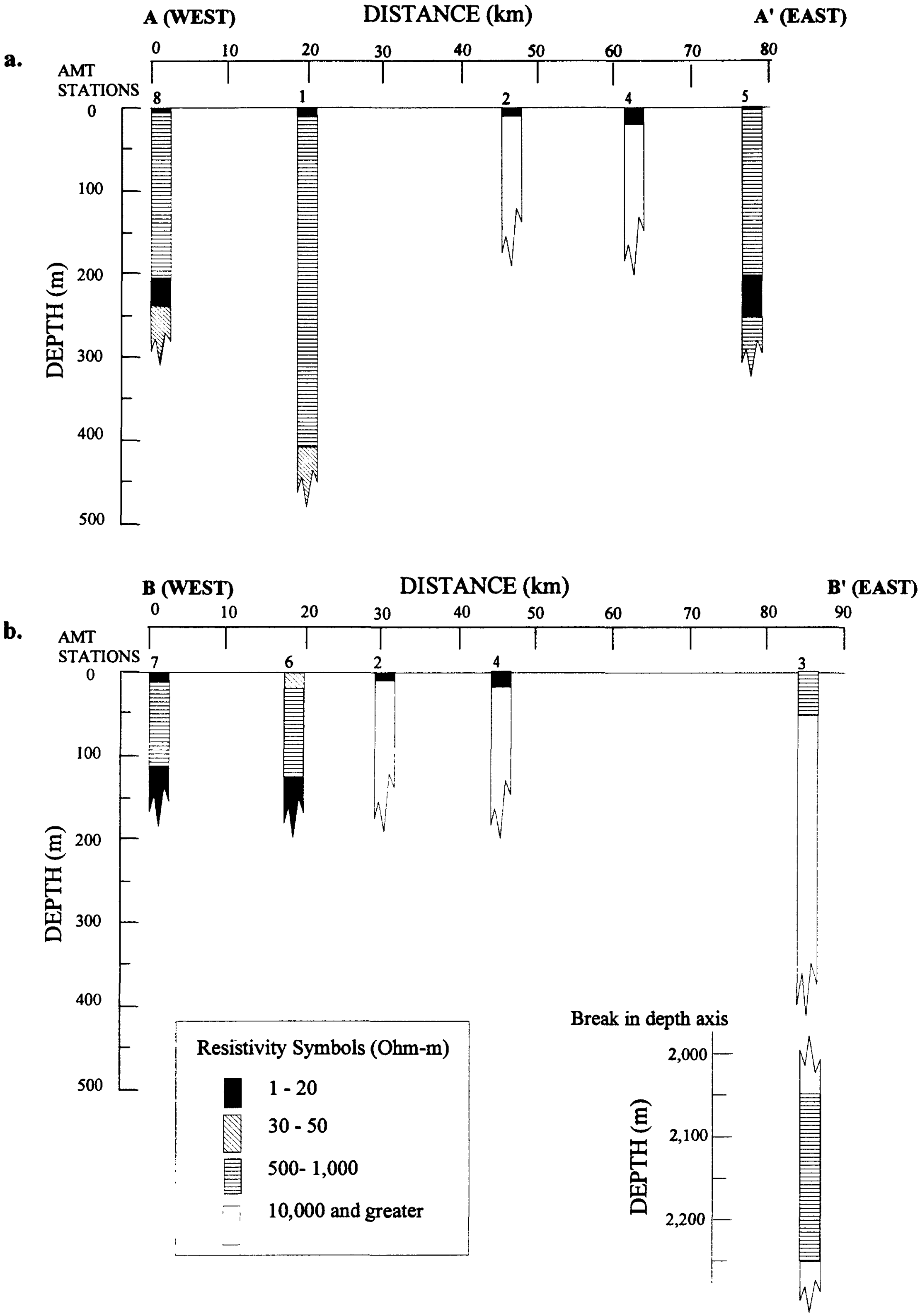

Figure 2 -- Resistivity versus depth sections for AMT soundings in the Cornudas Mountains area, southern New Mexico. Stations are graphed as: **a.** profile A-A', and **b.** profile B-B'; profile locations are shown on Figure 1. Soundings 2 and 4 are common to both profiles. Depth and resistivity parameters are listed in Table 1; sounding curves are shown in the appendix.

Stations 2 and 4 are unreliable in quantifying the parameters of layered resistivity (Table 1 and Appendix). Identified cultural noise sources in the area that may have reduced the reliability of there stations were buried telephone lines, and minor 2 or 3 wire power lines; these lines were are at least 100 m distant from measurements at sites 2 and 4. Wind is another noise source; there were moderate winds (5-15 mph estimated) when station 2 was observed, but station 4 was observed in calm conditions. Care was taken in setup at station 2 to minimize coil and wire vibrations due to the wind; it is thought that the moderate winds should not have been the major source of the bad data. Cultural noise signals were apparently the primary source of poor data at stations 2 and 4, and were probably not significantly attenuated in propagating from their source to the observation site. The inferred low attenuation itself suggests a more resistive subsurface than at other stations equally distance from such cultural features, such as stations 1 and 5. If the inference is correct, the resistivity may be in the high thousands of Ohm-m. Such a resistivity (say 10,000 Ohm-m) would be consistent with a shallow laccolith or thick sill.

Station 5, in the southeast part of the study area, about five km southeast of Black Mountain, and station 3, about 13 km east of Cornudas Mountain, are unique because they both indicate a resistive 4th layer beneath the conductive 3rd layer. Such conductive zones form the basal part of the detected resistivity in other soundings here. However, there is no assurance that the 3rd conductive layer of these stations 3 and 5 corresponds to the geology of the conductive layers elsewhere. The resistivity beneath sounding 3 is indicated to be much higher than any of the previously discussed data. It is probable that the sub-surface on the east flank of the Cornudas Mountains is unlike that on the west flank, and a difference in lithology, or structure must occur east of Black and Cornudas Mountains across a zone less than 8 km wide. This agrees with an interpreted geologic section (Black, 1975; King and Harder, 1985) which shows the pre-Permian section to be intensely faulted in the area east of Cornudas Mountains.

SUMMARY

Resistivity data acquired across the area of the Cornudas Mountains based on measurements of naturally occurring electromagnetic fields show some broad geoelectric features that have geologic implications for studies of the resource and environmental aspects of this area. The strata here are generally conductive (5-50 Ohm-m) at the depth range of a few meters to a few 10's of meters, but increase to thousands of Ohm-m below this surface zone. The resistive zone is usually about 100 to 200 m thick after which conductive rock (1-30 Ohm-m)is again sensed. Data from most of the observation sites could not penetrate beneath the 3rd conductive layer, but at soundings on the east flank of the study area, the data did see through the 3rd layer, and encountered high resistivity again. The differences between data on the east and west flanks of the Cornudas Mountains suggests a structural or lithological change in the subsurface east of Black Mountain and Cornudas Mountain.

In the western part of the Cornudas Mountains, inferences based on the present data and drill-hole information (Black, 1975; King and Harder, 1985) indicate that the upper 100-200 m of rock consists of Permian carbonates, weathered to be conductive at the top, and marked by conductive mudstone or shale at the base. Based on this inference, it is likely that the increased thickness of the resistive 2nd layer north of Flat Top Mountain (stations 6 and 7, Figure 1), and toward Cornudas Mountain from station 8, may indicate a flexure, or sill intrusion, or both, in the 2nd layer surrounding Cornudas Mountain.

REFERENCES

Black, B.A., 1975, Geology and oil and gas potential of the northeast Otero platform area, New Mexico; New Mexico Geological Society Guidebook 26, p.323-332

Cordell, Lindreth, 1983, Composite residual total intensity aeromagnetic map of New Mexico, available from the National Oceanic and Atmospheric Administration (NOAA), National Geophysical Data Center, Code E/GCI, 325 Broadway, Boulder, CO, 80303.

Hoover, D.B. and Long, C.L., 1976, Audio-magnetotelluric methods in reconnaissance geothermal exploration: Proc. 2nd United Nations Symposium on Development of Geothermal Resources, v. 2, p.1059-1064.

Hoover, D.B., Long, C.L. and Senterfit, R.M., 1978, Some results from audiomagnetotelluric investigations in geothermal areas. Geophysics, v.43, p.1501-1514.

King, W.E. and Harder, V.M., 1985, Oil and gas potential of the Tularosa basin-Otero platform-Salt Basin graben area, New Mexico and Texas: Socorro, New Mexico Bureau Mines Mineral Resources Circular 198, 36 p.

Madden, Theodore and Nelson, Phillip, 1985, A defense of Cagniard's magnetotelluric method, in Vozoff, Keeva, ed., Magnetotelluric methods, Geophysics Reprint Series No. 5: Tulsa, Society of Exploration Geophysicists, p.89-102.

McLemore, V.T. and Guilinger, J.R., 1995, Geology and mineral resources of the Cornudas Mountains, Otero County, New Mexico and Hudspeth County, Texas: Socorro, New Mexico Geological Society Guidebook 44th Field Conference, p.145-153.

Strangway, D.W., Swift, C.M. and Holmer, R.C, 1973, The application of audio-frequency magnetotellurics (AMT) to mineral exploration: Geophysics v.38, p.1159-1175.

U.S. Bureau of Mines, 1994, Mineral investigation of areas of critical environmental concern in part of the Caballo Resource Area, Otero County, New Mexico. U.S. Bureau Mines Mineral Land Assessment Open-file Report 20-94, 15 p.

Vozoff, Keeva, 1972, The magnetotelluric method in the exploration of sedimentary basins: Geophysics, v. 37, p.98-141.

Vozoff, Keeva, 1991, The magnetotelluric method; in Nabighian, M.N., ed., Electromagnetic methods in applied geophysics, v.2, Applications, Part B: Tulsa, Society of Exploration Geophysicist, p.641-711.

Wait, J.R., 1962, Theory of magnetotelluric fields: Journal of Research of the National Bureau of Standards-D, Radio Propagation, v. 66D, p.509-541.

APPENDIX

AMT Sounding Plots: Cornudas Mountains, southern New Mexico

Apparent resistivity versus frequency plots are provided for the audiomagnetotelluric stations in the area of the Cornudas Mountains. The stations designations are CF01 - CF08, where CF represents the USGS 1:100,000-scale Crow Flats quadrangle that contains these stations.

The top 2 graphs on each page shows the results of data processing: apparent resistivity (upper graph), phase estimates (middle graph), and error bars at each frequency for the two orthogonal modes (Ex:Hy and Ey:Hx). Error bars display the total spread of the estimates from different data series. The ordinate (vertical axis or Y) is apparent resistivity in Ohm-m (upper graph), or impedance (E/H) phase in degrees (lower graph). The abscissa (horizontal axis or X) is frequency in Hz. Apparent resistivity is plotted with log-log scaling; phase is plotted with a linear-log scaling. Triangles (T) represent estimates of apparent resistivity (Rxy) and phase (Pxy) from Ex:Hy components; boxes (B) represent estimates of apparent resistivity (Ryx) and phase (Pyx) from Ey:Hx components. The x and y directions are magnetic north and east respectively; the estimates are unrotated.

The bottom graph shows the data points, plotted along with the theoretical data curve for the layered model indicated. The phase data in this plot are fit into the lowest log-cycle, where the vertical range of the log-cycle is 90 degrees. In this plot, when phase values fall outside of the range of 0 to 90 degrees, the values are plotted at the extremes of the plot range (0 or 90 degrees). The axes, scalings, and triangle and box symbols follow the convention described for the upper and middle graphs. The phase scale in the bottom graph, plotted as a log-cycle is wrong; the phase data are plotted linearly from 0 to 90 degrees.

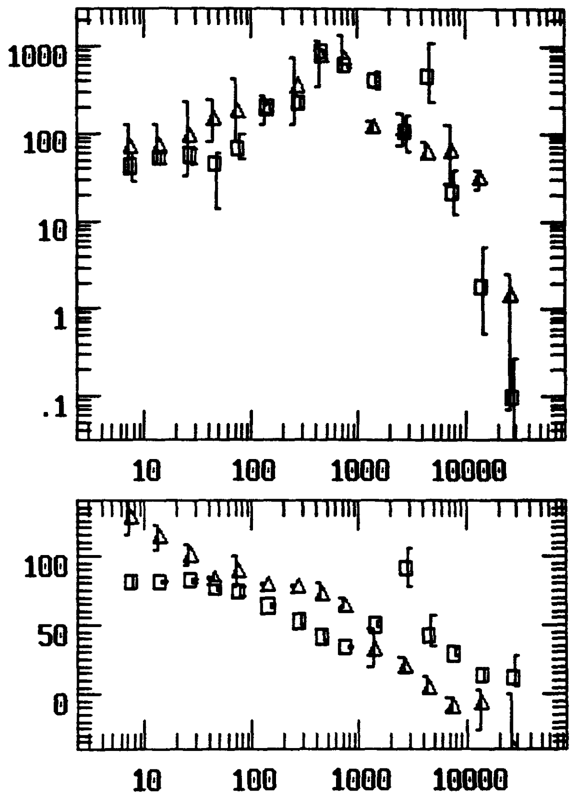

* C:\MTDATA\cf01

X:Log Freq.(Hz)
upper Y:Log App.Resis.: T:Rxy, B:Ryx
lower Y:Lin.Imp.Phase: T:Pxy, B:Pyx

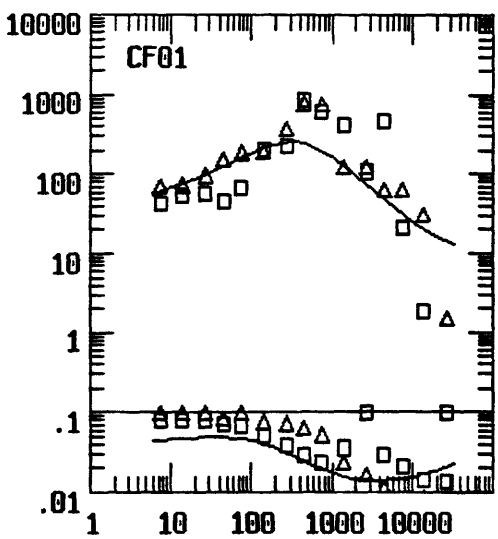

Layer:	Resis., (Ohm-m)	thick. (km)
1 :	15,.01	
2 :	1000,.4	
3 :	30,999	

X: Freq. (Hz)
Upper Y: App.Resis.(ohm-m)
Lower Y: Phase (90 deg.:1 cycle)

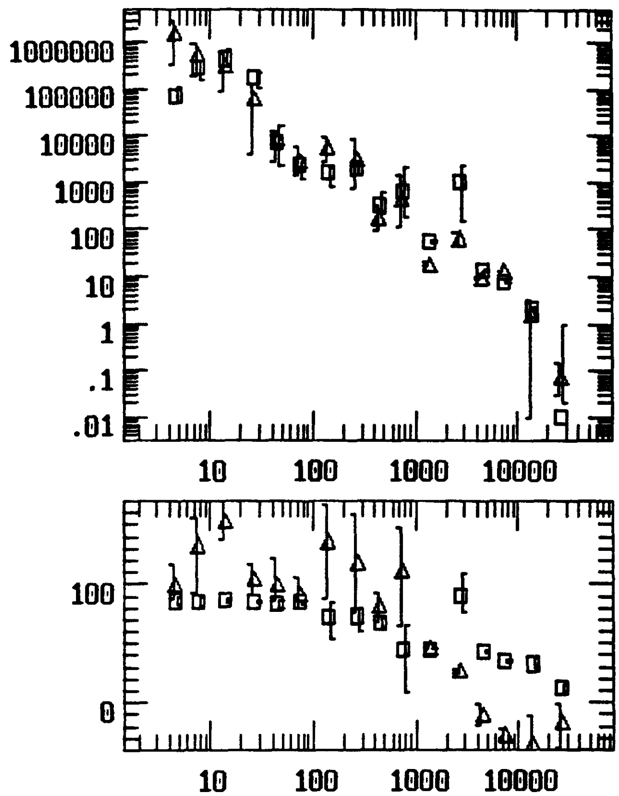

* C:\MTDATA\cf02

X:Log Freq.(Hz)
upper Y:Log App.Resis.: T:Rxy, B:Ryx
lower Y:Lin.Imp.Phase: T:Pxy, B:Pyx

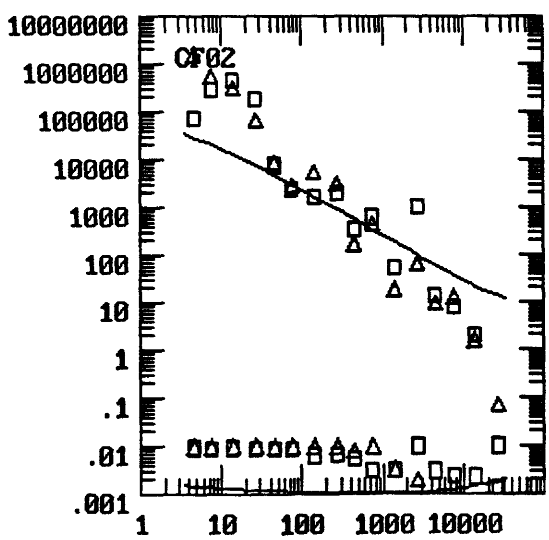

Layer: Resis., thick.
(Ohm-m) (km)
1 : 15, .01
2 : 200000,999

X: Freq. (Hz)
Upper Y: App.Resis.(ohm-m)
Lower Y: Phase (90 deg.:1 cycle)

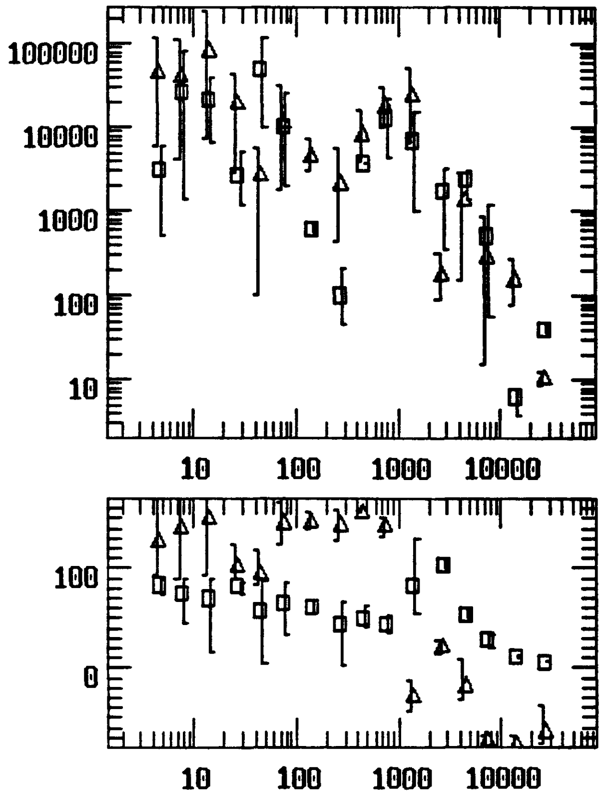

* C:\MTDATA\cf03

X:Log Freq.(Hz)
upper Y:Log App.Resis.: T:Rxy, B:Ryx
lower Y:Lin.Imp.Phase: T:Pxy, B:Pyx

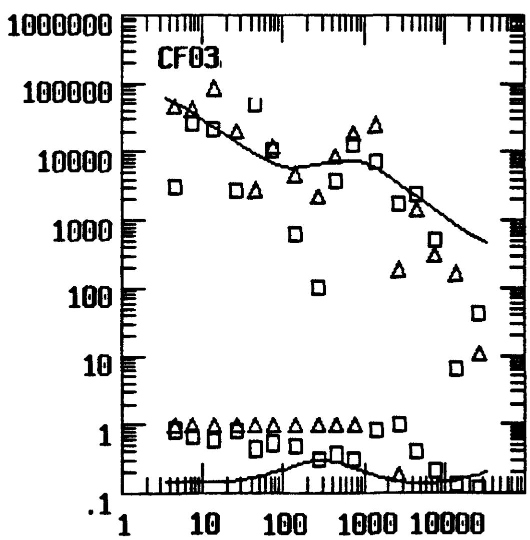

X: Freq. (Hz)
Upper Y: App.Resis.(ohm-m)
Lower Y: Phase (90 deg.:1 cycle)

Layer:	Resis., (Ohm-m)	thick. (km)
1 :	500,	.05
2 :	50000,	2
3 :	500,	.2
4 :	500000,	999

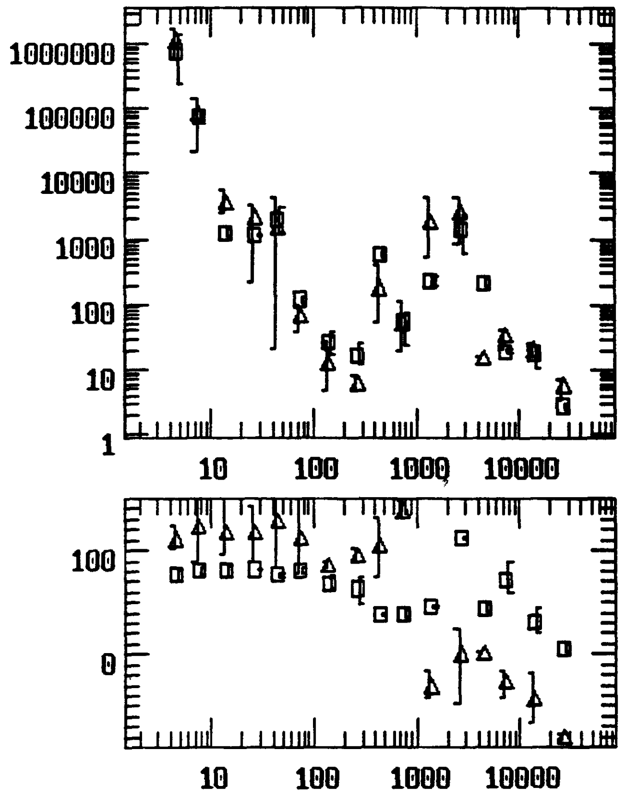

* C:\MTDATA\cf04

X:Log Freq.(Hz)
upper Y:Log App.Resis.: T:Rxy, B:Ryx
lower Y:Lin.Imp.Phase: T:Pxy, B:Pyx

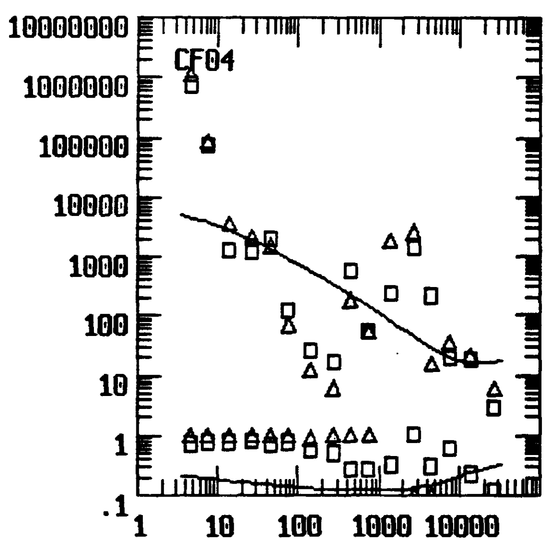

X: Freq. (Hz)
Upper Y: App.Resis.(ohm-m)
Lower Y: Phase (90 deg.:1 cycle)

Layer:	Resis., (Ohm-m)	thick. (km)
1 :	20,.02	
2 :	10000,999	

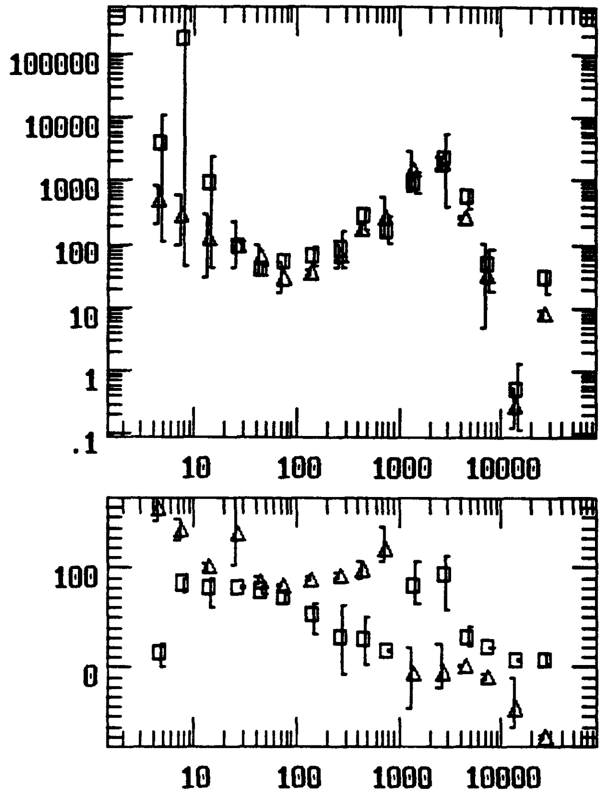

* C:\MTDATA\cf05

X:Log Freq.(Hz)
upper Y:Log App.Resis.: T:Rxy, B:Ryx
lower Y:Lin.Imp.Phase: T:Pxy, B:Pyx

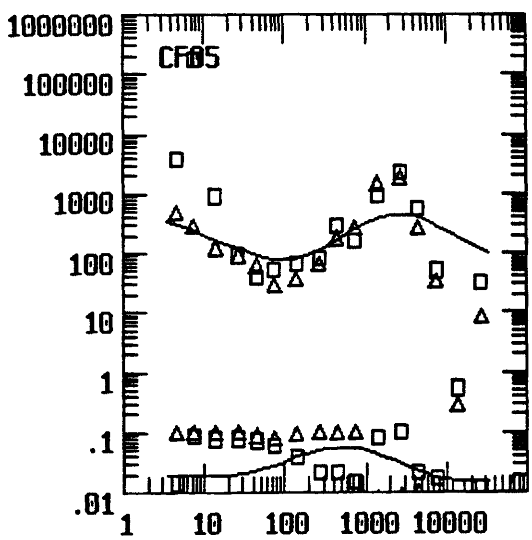

Layer:	Resis., (Ohm-m)	thick. (km)
1 :	20,	.003
2 :	1000,	.2
3 :	10,	.05
4 :	1000,	999

X: Freq. (Hz)
Upper Y: App.Resis.(ohm-m)
Lower Y: Phase (90 deg.:1 cycle)

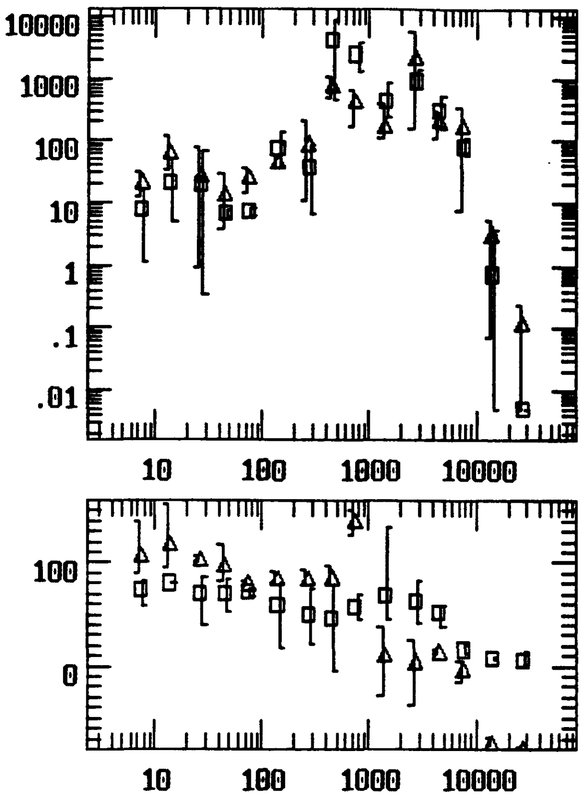

* C:\MTDATA\cf06

X:Log Freq.(Hz)
upper Y:Log App.Resis.: T:Rxy, B:Ryx
lower Y:Lin.Imp.Phase: T:Pxy, B:Pyx

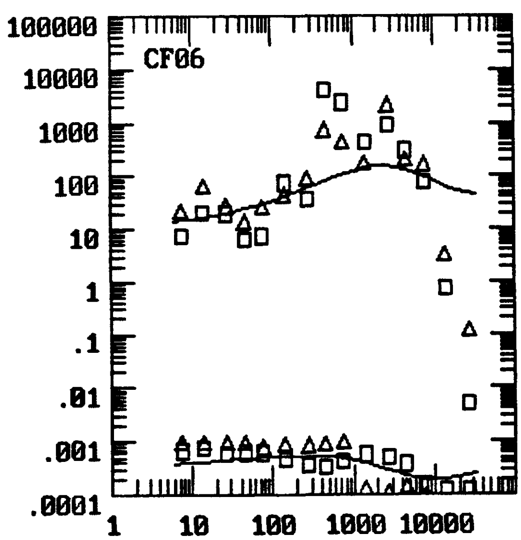

Layer:	Resis., (Ohm-m)	thick. (km)
1 :	50,	.02
2 :	1000,	0.1
3 :	10,	999

X: Freq. (Hz)
Upper Y: App.Resis.(ohm-m)
Lower Y: Phase (90 deg.:1 cycle)

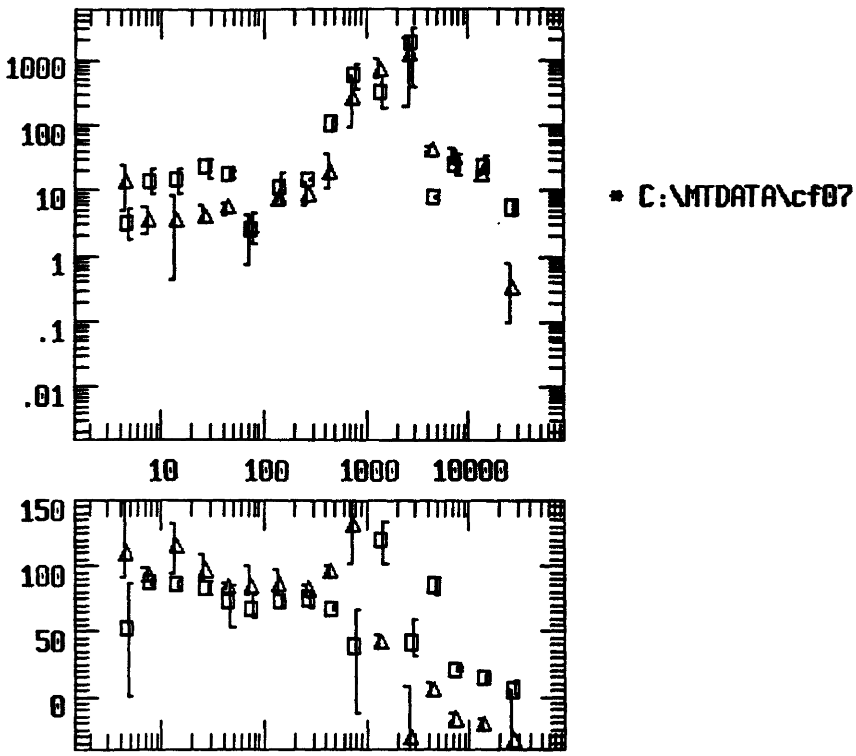

X:Log Freq.(Hz)
upper Y:Log App.Resis.: T:Rxy, B:Ryx
lower Y:Lin.Imp.Phase: T:Pxy, B:Pyx

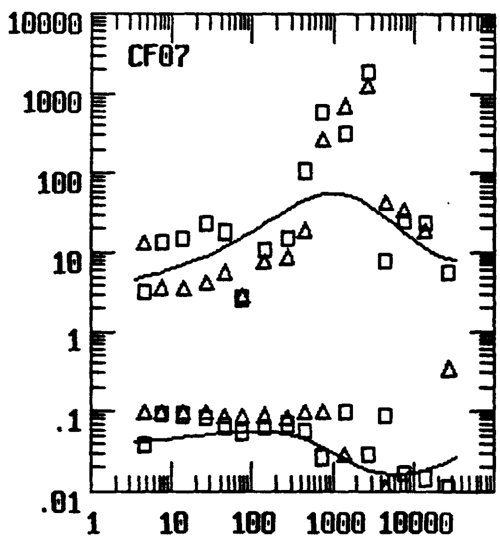

X: Freq. (Hz)
Upper Y: App.Resis.(ohm-m)
Lower Y: Phase (90 deg.:1 cycle)

Layer:	Resis., (Ohm-m)	thick. (km)
1 :	10,.01	
2 :	1000,.1	
3 :	3,999	

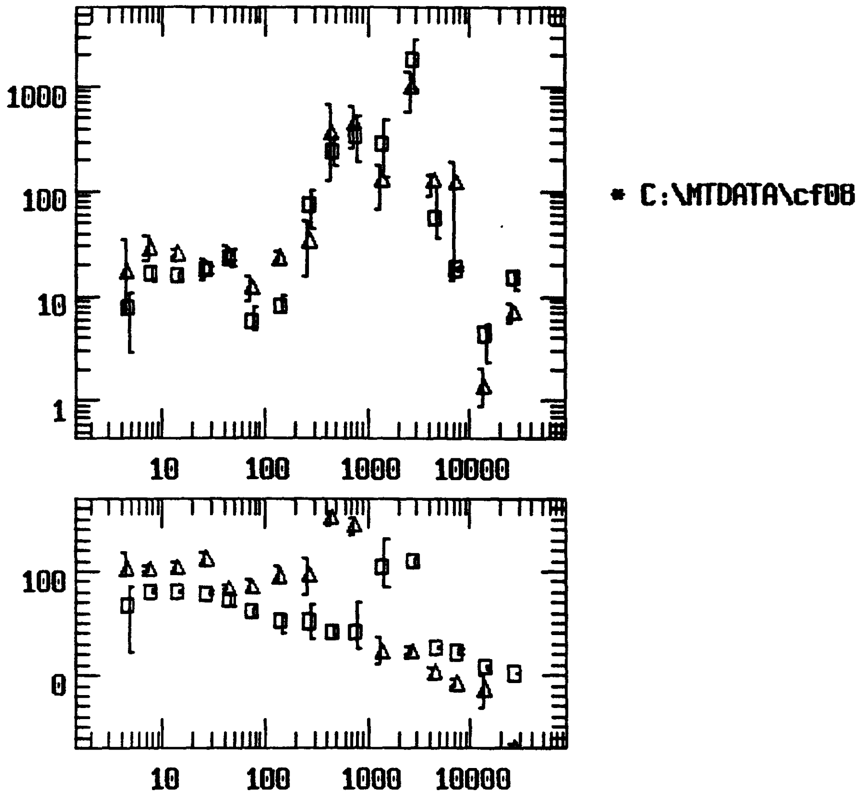

X:Log Freq.(Hz)
upper Y:Log App.Resis.: T:Rxy, B:Ryx
lower Y:Lin.Imp.Phase: T:Pxy, B:Pyx

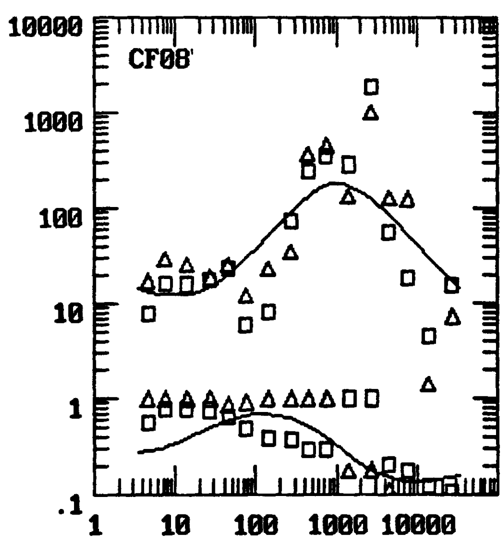

Layer:	Resis., (Ohm-m)	thick. (km)
1 :	10,	.005
2 :	1000,	.2
3 :	1,	.03
4 :	30,	999

X: Freq. (Hz)
Upper Y: App.Resis.(ohm-m)
Lower Y: Phase (90 deg.:1 cycle)